Reduction of mode partition noise of FP-LD by using Mach-Zehnder interferometer for RSOA-based DWDM applications

Sang-Hwa Yoo,[1,2] Sang-Rok Moon,[1] Myeonggyun Kye,[1] and Chang-Hee Lee[1,*]

[1]*Department of Electrical Engineering, Korea Advanced Institute of Science and Technology, 291 Daehak-ro, Yuseong-gu, Daejeon, 34141, South Korea*

[2]*Currently with the Optical Internet Research Department, Electronics and Telecommunications Research Institute, 218 Gajeong-ro, Yuseong-gu, Daejeon, 34129, South Korea*

[*]*changheelee@kaist.edu*

Abstract: We investigate reduction of mode partition noise of a spectrally sliced Fabry-Perot laser diode (FP-LD) for application to seeded DWDM systems. The proposed scheme for the noise reduction incorporates a fiber-based Mach-Zehnder interferometer (MZI) and a reflective semiconductor optical amplifier (RSOA). The MZI enables to reduce a relative intensity noise (RIN) more than 3 dB with better noise distributions. Experimental results of 10-Gb/s signal transmission exhibit a considerable bit-error-rate (BER) reduction by three orders of magnitude at the given received power. After the noise reduction, the FP-LD is applied to a 10-Gb/s DWDM system as a seed-light-source. In a local-seeding scheme, return-to-zero (RZ) and carrier-suppressed (CS)-RZ signal formats are compared as a function of transmission distance. Furthermore, a back-reflection induced impairment is evaluated in a remote-seeding scheme. We also count the number of useable channels to show the feasibility of DWDM transmission.

OCIS codes: (060.4510) Optical communications; (060.4250) Networks.

References and links

1. A. D. McCoy, P. Horak, B. C. Thomsen, M. Ibsen, and D. J. Richardson, "Noise suppression of incoherent light using a gain-saturated SOA: implications for spectrum-sliced WDM systems," J. Lightwave Technol. **23**(8), 2399–2409 (2005).
2. H. D. Kim, S.-G. Kang, and C.-H. Lee, "A low-cost WDM source with an ASE injected Faby-Pérot semiconductor laser," IEEE Photonics Technol. Lett. **12**(8), 1067–1069 (2000).
3. F. Payoux, P. Chanclou, M. Moisnard, and R. Brenot, "Gigabit optical access using WDM PON based on spectrum slicing and reflective SOA," in *Proc. of ECOC 2005* (2005), paper We 3.3.5.
4. H. Kim, "Pulsed-incoherent-light-injected Fabry-Perot laser diode for WDM passive optical networks," Opt. Express **18**(2), 1714–1721 (2010).
5. J.-Y. Kim, S.-H. Yoo, S.-R. Moon, D. C. Kim, and C.-H. Lee, "400 Gb/s (40 × 10 Gb/s) ASE injection seeded WDM-PON based on SOA-REAM," in *Proc. of OFC/NFOEC 2013* (2013), paper OW4D.
6. S.-H. Yoo, S.-R. Moon, M. Kye, and C.-H. Lee, "Pulsed-ASE-seeded DWDM optical system with interferometric noise suppression," Opt. Express **22**(7), 8790–8797 (2014).
7. Z. G. Lu, J. R. Liu, P. J. Poole, S. Raymond, P. J. Barrios, D. Poitras, G. Pakulski, X. P. Zhang, K. Hinzer, and T. J. Hall, "Low noise InAs/InP quantum dot C-band monolithic multiwavelength lasers for WDM-PONs," in *Proc. of OFC/NFOEC 2009* (2009), paper JWA27.
8. A. Akrout, A. Shen, R. Brenot, F. Van-Dijk, O. Legouezigou, F. Pommereau, F. Lelarge, A. Ramdane, and G.-H. Duan, "Separate error-free transmission of eight channels at 10 Gb/s using comb generation in a quantum-dash-based mode-locked laser," IEEE Photonics Technol. Lett. **21**(23), 1746–1748 (2009).
9. M. Gay, A. O'Hare, L. Bramerie, Z. Hao, S. Fresnel, C. Peucheret, P. Besnard, S. Joshi, S. Barbet, and F. Lelarge, "Single quantum dash mode-locked laser as a comb-generator in four-channel 112 Gbit/s WDM transmission, " in *Proc. of OFC 2014* (2014), paper Tu2H.5.
10. S.-G. Mun, H.-S. Cho, and C.-H. Lee, "A Cost-Effective WDM-PON Using a Multiple Section Fabry–Pérot Laser Diode," IEEE Photonics Technol. Lett. **23**(1), 3–5 (2011).
11. K. Sato and H. Toba, "Reduction of mode partition noise by using semiconductor optical amplifiers," IEEE J. Sel. Top. Quantum Electron. **7**(2), 328–333 (2001).

#268199 Received 13 Jun 2016; accepted 14 Jun 2016; published 17 Jun 2016

12. X. Xue, X. Zheng, H. Zhang, and B. Zhou, "Noise suppression for fiber radio transmission on spectrum-sliced WDM-PONs employing interferometric structures," in *Proc. of OFC/NFOEC 2011* (2011), paper OWK6.
13. S.-H. Yoo, J.-Y. Kim, B.-I. Seo, and C.-H. Lee, "Noise-suppressed mutually injected Fabry-Perot laser diodes for 10-Gb/s broadcast signal transmission in WDM passive optical networks," Opt. Express **21**(5), 6538–6546 (2013).
14. S.-R. Moon, S.-H. Yoo, and C.-H. Lee, "Effect of noise distribution in a WDM system seeded by a spectrum-sliced ASE," J. Lightwave Technol. **32**(12), 2271–2276 (2014).
15. Y. Okano, K. Nakagawa, and T. Ito, "Laser mode partition noise evaluation for optical fiber transmission," IEEE Trans. Commun. **28**(2), 238–243 (1980).
16. "G.975: Forward error correction for submarine systems," Recommendation, ITU-T (2000).
17. F. Koyama and K. Oga, "Frequency chirping in external modulators," J. Lightwave Technol. **6**(1), 87–93 (1988).
18. A. X. Widmer and P. A. Franaszek, "A DC-balanced, partitioned-block, 8B/10B transmission code," IBM J. Res. Develop. **27**(5), 440–451 (1983).
19. G. Charlet, "Progress in optical modulation formats for high-bit rate WDM transmissions," IEEE J. Sel. Top. Quantum Electron. **12**(4), 469–483 (2006).
20. P. Winzer and R. Essiambre, "Advanced optical modulation formats," Proc. IEEE **94**(5), 952–985 (2006).
21. V. Wongpaibool, J. K. Shaw, and I. Jacobs, "Comparison of alternative carrier-suppressed return-to-zero modulation formats," Proc. SPIE **5247**, 284–298 (2003).
22. D. C. Kim, H.-S. Kim, K. S. Kim, B.-S. Choi, J.-S. Jeong, and O.-K. Kwon, "10 Gbps SOA-REAM using monolithic integration of planar buried-heterostructure SOA with deep-ridge waveguide EA modulator for colourless optical source in WDM-PON," in *Proc. of ECOC 2011*, paper Tu.5.LeSaleve.5.
23. C. H. Kim, "Performance evaluation of reflective electro-absorption modulator based optical source using a broadband light seed source for colorless WDM-PON applications," Opt. Express **21**(10), 12914–12919 (2013).
24. J.-H. Moon, K.-M. Choi, S.-G. Mun, and C.-H. Lee, "Effects of back-reflection in WDM-PONs based on seed light injection," IEEE Photonics Technol. Lett. **19**(24), 2045–2047 (2007).
25. K. Morito, M. Ekawa, T. Watanabe, and Y. Kotaki, "High-output-power polarization-insensitive semiconductor optical amplifier," J. Lightwave Technol. **21**(1), 176–181 (2003).
26. K. Iwashita and K. Nakagawa, "Mode partition noise characteristics in high-speed modulated laser diodes," IEEE J. Quantum Electron. **18**(12), 2000–2005 (1982).
27. K. Tanaka, A. Agata, and Y. Horiuchi, "IEEE 802.3av 10G-EPON standardization and its research and development status," J. Lightwave Technol. **28**(4), 651–661 (2010).
28. J. J. Carr, S. L. Saikkonen, and D. H. Williams, "Refractive index measurements on single-mode fiber as functions of product parameters, tensile stress, and temperature," Fiber Integr. Opt. **9**(4), 393–396 (1990).
29. S. H. Bae, H. K. Shim, U. H. Hong, H. Kim, A. Agata, K. Tanaka, M. Suzuki, and Y. C. Chung, "25-Gb/s TDM optical link using EMLs for mobile fronthaul network of LTE-A system," IEEE Photonics Technol. Lett. **27**(17), 1825–1828 (2015).
30. J. Wei, N. Eiselt, H. Griesser, K. Grobe, M. H. Eiselt, J. J. V. Olmos, I. T. Monroy, and J.-P. Elbers, "Demonstration of the first real-time end-to-end 40-Gb/s PAM-4 for next-generation access applications using 10-Gb/s transmitter," J. Lightwave Technol. **34**(7), 1628–1635 (2016).

1. Introduction

In recent years, the drastic growth in bandwidth-intensive applications has been driving multi-gigabit sustained bit-rate services for optical access/metro networks. To meet the huge capacity demand, a dense wavelength division multiplexing (DWDM) based on spectral filtering of broadband incoherent [1–6] or coherent [7–11] light sources has been intensively studied. In particular, a seeded DWDM system based on an amplified-spontaneous-emission (ASE) light can be realized in a cost-effective manner [2–6]. For a colorless operation, each optical transmitter is equipped with a wavelength independent reflective modulator such as an anti-reflection coated Fabry-Perot laser diode (FP-LD) or a reflective semiconductor optical amplifier (RSOA). The reflective modulator also acts as a limiting amplifier to suppress intensity fluctuations arising from ASE-ASE beat noise. However, residual intensity noise in high frequencies still restricts an achievable bit-rate-per-channel. On the other hand, quantum dot/dash mode locked lasers (QD-MLLs) can enable a high-speed transmission over 10-Gb/s due to low amplitude and phase noise [8,9]. However, these lasers are based on rather costly and complex manufacturing process. As an economical alternative, continuous wave quantum well (QW) FP-LDs have been considered [10,11]. However, a major limitation of the QW-based lasers is relative intensity noise (RIN) at low-frequency region of a selected individual mode, so-called "mode partition noise". It is even difficult to transmit signals at 1.25-Gb/s without noise reduction techniques [10]. This limitation has been mitigated by using a gain-

#268199 Received 13 Jun 2016; accepted 14 Jun 2016; published 17 Jun 2016

saturated SOA (or RSOA) in the same as the ASE-ASE beat noise suppression. However, it requires a high injection power (≥10 dBm) for sufficient noise suppression [11].

In this paper, we propose a simple technique to reduce the mode partition noise by employing a fiber-based Mach-Zehnder interferometer (MZI). The ability of the MZI to reduce the intensity noise has been reported for an ASE light source and a mutually injected FP-LDs [12,13]. However, reduction of the mode partition noise appearing at low frequencies has not been clarified. To do this, we exploit the MZI with a long-time delay exhibiting low-noise windows at intervals of a few tens of megahertz unlike previous demonstrations. Furthermore, we analyze effects of the MZI with the gain-saturated RSOA through measurement of statistical noise distributions and RIN spectra. We found that the MZI enables to not only reduce the mode partition noise itself, but also lead an enhancement of the noise suppression by the gain-saturated RSOA. We present bit-error-rate (BER) results of 10-Gb/s signal to show an impact of the MZI on a transmission performance.

The noise-reduced FP-LD is then applied to an injection seeded DWDM system as a seed-light-source for demonstrating the 10-Gb/s signal transmission without dispersion compensation. We investigate a chromatic dispersion effect on the two kinds of seeding schemes, a local- and remote-seeding. For each scheme, a suitable modulation method is suggested among a non-return-to-zero (NRZ), optically/electrically generated RZ, and carrier-suppressed (CS)-RZ signal according to transmission distance. Furthermore, in the remote-seeding scheme, a back-reflection induced impairment and usable DWDM channel is also discussed.

2. Proposed technique for reduction of mode partition noise

2.1 Reduction of mode partition noise by using MZI

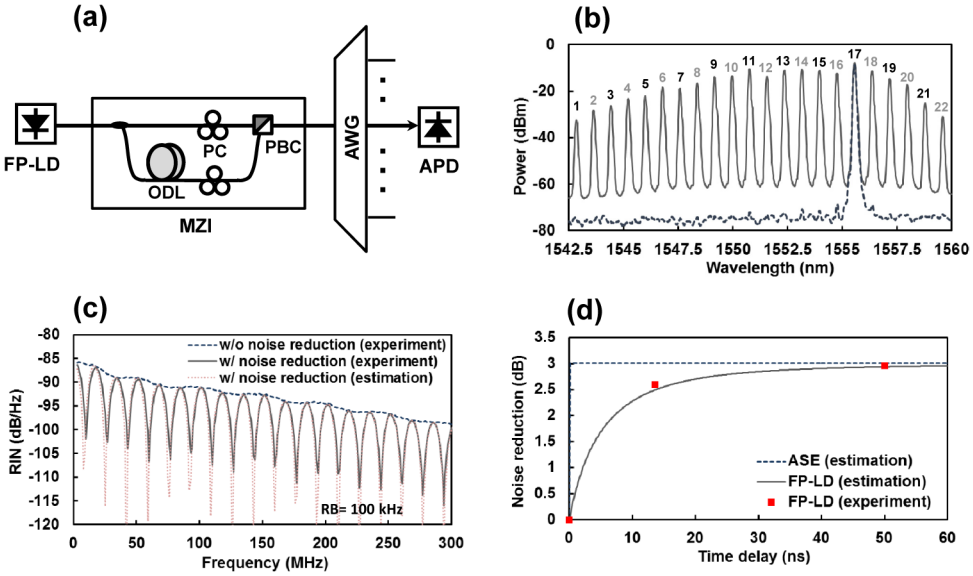

Fig. 1. (a) Schematics of the noise reduction measurement for the FP-LD based on the MZI, (b) optical spectrum of all modes and a single filtered mode, (c) RIN spectra of a single filtered mode (#17), and (d) noise reduction ratio vs time delay.

Figure 1(a) shows a schematic diagram for noise reduction measurement of an FP-LD with the MZI. The FP-LD has an InP-based QW active region with a cavity length of 420 μm. A bias current and operating temperature were set to be 200 mA (The threshold current was 40 mA.) and 20 °C, respectively. Figure 1(b) shows measured optical spectrum of all modes and a single filtered mode under these conditions. We can see more than 20 lasing modes with a

#268199 Received 13 Jun 2016; accepted 14 Jun 2016; published 17 Jun 2016

mode spacing of 100 GHz (0.8 nm). Each mode was spectrally sliced by a conventional flat-top type arrayed-waveguide grating (AWG). A channel spacing of the AWG was 100 GHz (0.8 nm). A 3-dB and 1-dB bandwidth were 80 GHz (0.64 nm) and 50 GHz (0.4 nm), respectively. Likewise, the AWG has a very flat transmission so that a less strict fabrication requirement of the FP-LD is required in terms of mode spacing compared to Gaussian type AWGs. By adopting a thermoelectric cooler (TEC) of the FP-LD, lasing wavelengths are matched with center wavelengths of the AWG, respectively. RIN spectrum of a single filtered mode (#17 mode was selected in our measurement) was measured by using an avalanche photo diode (APD) and an electrical spectrum analyzer (ESA). The APD has a bandwidth of 6 GHz and the ESA has a resolution bandwidth (RB) of 100 kHz. With an average count of 50 times, we could obtain a consistent experimental result (blue dashed line) as shown as in Fig. 1(c). It has a peak at dc and monotonically decreases with increase of the frequency. A 3-dB bandwidth of the mode partition noise was measured to be 33 MHz.

For reduction of the mode partition noise, we introduce a MZI with a long-time delay as depicted in Fig. 1(a). After a beam splitter, two streams of light with the same intensity are orthogonally polarization-combined by using a polarization controller (PC) for each arm of the MZI and a polarization beam combiner (PBC). Here, two streams of light have a time delay difference by inserting an optical delay line (ODL) to one of arms. After spectrum slicing, those intensity fluctuations induced by the mode partition noise interfere with each other at the APD. As seen in Fig. 1(c), the MZI was able to reduce the RIN creating a series of low-noise windows (black solid line). The first low-noise window was measured around 10 MHz corresponding to the time delay of 50 ns. The RIN spectrum with interferometric noise suppression is given by [12],

$$RIN_{wMZI}(f) = \frac{1}{2} \times \left(1 + \cos\left(2\pi f \Delta\tau\right)\right) \times RIN_{woMZI}(f) \tag{1}$$

where, f is the frequency, $\Delta\tau$ is the time delay difference of the MZI, and $RIN_{woMZI}(f)$ is the measured RIN spectrum of the mode partition noise. We estimated RIN spectrum after noise reduction (red dotted line) and the result is in a good agreement with the measured one.

As shown in Fig. 1(d), we also estimated a noise reduction ratio as a function of the time delay from 100 ps to 60 ns (100 ps time step) based on Eq. (1). The noise reduction ratio is enhanced with increasing the time delay and it would reach up to the maximum of 3 dB.

2.2 Impact of the MZI on noise suppression by RSOA

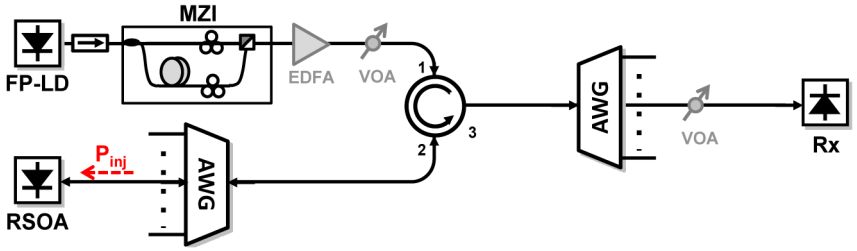

Fig. 2. Experimental setup for mode partition noise reduction using a MZI and a gain-saturated RSOA.

The RSOA (or SOA) also enables the mode partition noise suppression due to its gain saturation effect [9,11]. Thus, we assessed the feasibility of the noise reduction using both the MZI and the gain-saturated RSOA, simultaneously. As shown in Fig. 2, the orthogonally polarization-combined lights from the MZI were spectrally sliced by an AWG and injected to a polarization-insensitive TO-can type RSOA. A bias current of the RSOA was set to be 80 mA and its polarization dependent gain (PDG) was measured to be less than 0.3 dB. An

#268199 Received 13 Jun 2016; accepted 14 Jun 2016; published 17 Jun 2016

Erbium doped fiber amplifier (EDFA) and a variable optical attenuator (VOA) were inserted for varying the injection power to the RSOA (denoted as P_{inj} in Fig. 2). The light output of the RSOA passed through two AWGs and then delivered to the APD-based receiver.

We firstly measured an average RIN from 3- to 500-MHz according to the injection power to the RSOA as shown in Fig. 3(a). As the injection power increased from −18 dBm to −6 dBm without the use of the MZI, the average RIN was suppressed from −101.5 dB/Hz to −112.2 dB/Hz due to gain saturation of the RSOA (●). By inserting the MZI, the average RIN was reduced in all measurement range (■). It is noteworthy that the noise reduction attributed to the use of the MZI exceeds 3 dB unlike the previous RIN results of Fig. 1(d). For example, the difference was measured to be 4.4 dB for the injection power of −6 dBm having the average RIN of −116.6 dB/Hz. The inset of Fig. 3(a) displays the RIN reduction in spectral domain. We clearly observed the noise reduction even at the constructive interference peaks marked with black arrows. This result is unexpected because the interferometric noise reduction by the MZI only occurs in destructive interference as seen in the RIN spectra of Fig. 1(c).

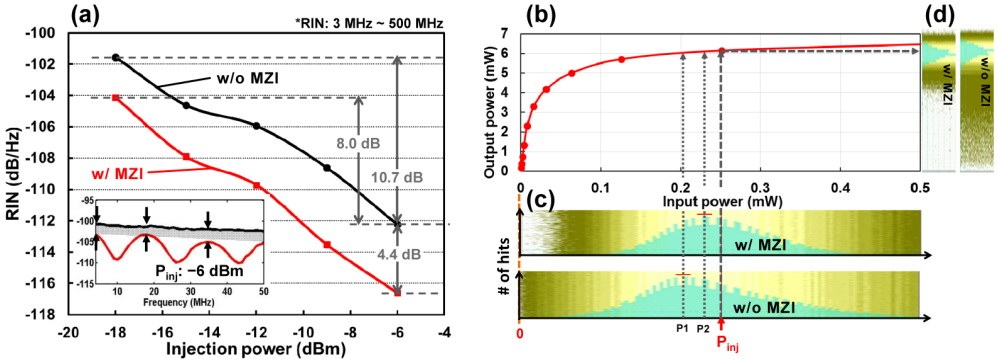

Fig. 3. (a) Measured average RIN, (b) input-power-versus-output-power curve of a RSOA, histograms of (c) input lights, and (d) output lights with and without a MZI. Inset in Fig. 3(a) shows RIN spectra at injection power of −6 dBm.

To figure out the additional noise reduction effect, we measured an input-power-versus-output-power characteristic of the RSOA. Figure 3(b) shows the saturation characteristic (nonlinear gain) of the RSOA, resulting in the noise suppression. In addition, we measured histograms of the input light of the RSOA with and without the MZI to investigate an effect of statistical noise distributions, since the noise distribution exerts a strong influence on RSOA-based systems [14]. The average input power of a sampling oscilloscope is kept the same for an accurate comparison. As illustrated in Fig. 3(c), both histograms reveal the asymmetric noise distribution as the mode partition noise (without the MZI) follows the Gamma function approximately [15]. However, with the MZI, the noise distribution has a shorter tail and the maximum number of hits is obtained at the much higher power [compare P1 for without the MZI and P2 for with the MZI in Fig. 3(c)] towards a mean value of −6 dBm [denoted as P_{inj}]. Thus, the input noises experience a stronger gain saturation effect resulting in more noise suppression as shown in Fig. 3(b). This is why the MZI achieves noise reduction more than 3 dB when it is used with the RSOA.

Furthermore, Fig. 3(d) displays a noticeable improvement of the noise distribution of the output light due to the MZI. Without the MZI, the RSOA cannot suppress the input long-tailed noise. However, the MZI makes the input noise distribution have a shorter tail so that the output intensity fluctuation can be significantly suppressed.

#268199 Received 13 Jun 2016; accepted 14 Jun 2016; published 17 Jun 2016

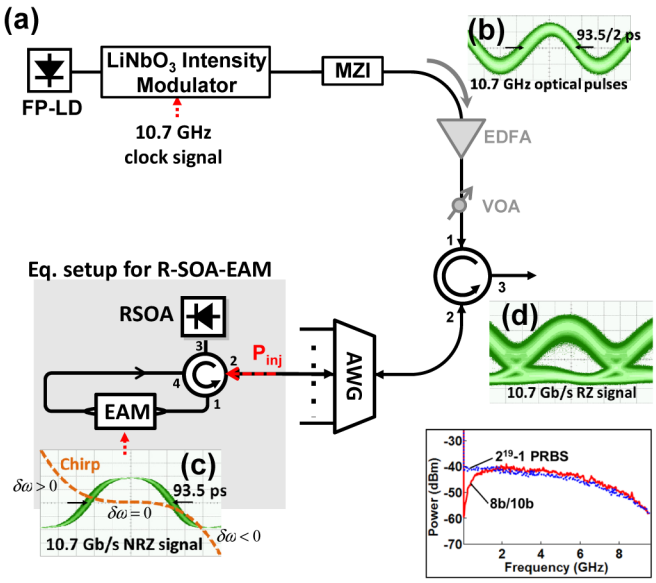

Fig. 4. (a) Schematics of an optical transmitter for BER measurement, (b) measured waveform of 10.7 GHz optical pulses after a $LiNbO_3$ intensity modulator and a MZI, (c) 10.7 Gb/s electrical NRZ signal at an EAM, and (d) 10.7 Gb/s optical RZ signal at a 3rd output port of circulator. Inset shows spectra of driving electrical PRBS and 8b/10b signals at an EAM.

We then assessed an effect of the MZI on the BER curves. The continuous lightwave from the FP-LD was modulated into optical pulses for the better transmission performance [4,6]. A single-drive $LiNbO_3$ intensity modulator acting as a pulse carver was inserted between the FP-LD and the MZI as shown in Fig. 4(a). The modulator which has a 3-dB bandwidth of 11.8 GHz was driven by a 10.7 GHz clock signal which has duty cycle of 50%. The time delay difference of the MZI should be a multiple of one pulse period (93.5 ps) around 50 ns. As illustrated in Fig. 4(b), a sinusoidal waveform of the optical pulse which has a temporal width of a half of one pulse period was measured at the output of the MZI. We confirmed that no differences were observed in the pulse waveform before and after the MZI.

After passing through an optical circulator, the pulsed-seed-light is spectrum-sliced into the individual FP cavity mode. Since the 100 GHz channel spaced AWG has a 3-dB bandwidth of 80 GHz (0.64 nm) much larger than clock frequency, it does not affect a temporal width of optical pulses. For the 10.7-Gb/s signal modulation, we consider a compact RSOA integrated with an electro-absorption modulator (R-SOA-EAM) as a high-speed reflective modulator [5]. However, due to the lack of this optical device in our experiment, we used an equivalent setup comprised of the RSOA and an EAM (CIP, 10G-LR-EAM-1550) and optical circulators as described in [6]. The used EAM has a typical 3-dB bandwidth of 14 GHz. A pseudorandom binary sequence (PRBS) signal has a pattern length of 2^{19}-1 and a bit-rate of 10.7 Gb/s includes an overhead of a standard forward error correction (FEC) code, Reed-Solomon (RS) (255, 239) [16]. As a consequence of inputting the optical pulses to the EAM, a RZ signal with a 50% duty cycle was generated (hereafter referred to as RZ50).

In this experiment, we found that the EAM inputted by the pulsed-seed-light would induce less frequency chirping [17] to the modulated signal. Figure 4(c) shows a driving NRZ signal which has a temporal width of 93.5 ps and calculated frequency chirp occurred in the EAM. The blue- and red-chirp occurs in the leading- and tailing-edge, respectively. However, it retains the zero-chirp in the middle of the NRZ signal. The temporal width of zero-chirp region is comparable with that of the inputted optical pulse (a half of 93.5 ps). Thus even though the low-cost EAM has a high chirp parameter of 1–2.5, it gives less frequency chirp to the modulated signal resulting in improvement of dispersion tolerance. This is why the output

#268199 Received 13 Jun 2016; accepted 14 Jun 2016; published 17 Jun 2016

light of the FP-LD was modulated into the optical pulses in this BER measurement with the cost of the pulse-carving. The eye diagram of Fig. 4(d) is measured at the 3rd output port of the three-port circulator and exhibits a 10.7 Gb/s optical RZ50 signal at the injection power of −6 dBm to the RSOA. After transmission over a 20-km-long single mode fiber (SMF), the BER curves were measured with and without the MZI.

In addition, dc-balanced 8b/10b line encoding was adopted for the further improvement [18]. The inset shows a negligible amount of signal spectrum around dc of the electrical 8b10b signal compared with that of the PRBS signal. It gives another chance to suppress the residual mode partition noise by means of an electrical high pass filter (HPF) at an optical receiver [13]. The optimum cutoff frequency of the optical receiver was found to be about 265 MHz through the BER measurements.

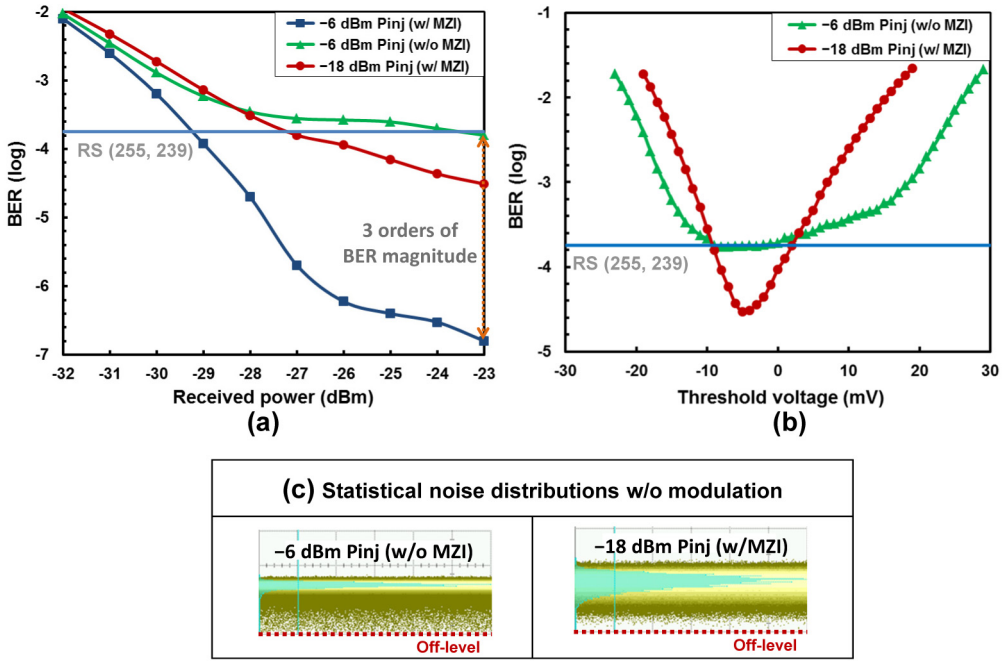

Fig. 5. (a) Measured BER curves of the 10.7-Gb/s optical RZ50 signals, (b) corresponding V-curves, and (c) statistical noise distributions w/o modulation.

Figure 5(a) shows the measured BER curves of the RZ50 signal according to injection power to the RSOA. Without the MZI, the FEC threshold is barely achievable even for the high injection power of −6 dBm (▲). However, the MZI dramatically improves the BER performance by three orders of magnitude at the received power of −23 dBm (■) due to the RIN reduction and noise distribution change as shown in Fig. 3(d). Interestingly, we observed even better BER for the injection power of −18 dBm (●), in spite of the worse RIN by 8.0 dB [see Fig. 3(a)]. To understand this, we measured the BER while changing a threshold voltage level at the optical receiver (such as so-called "V-curve measurement"). The received power was −23 dBm. As seen in Fig. 5(b), in comparison to the side parts of each curve, the green-triangles show the better BER than the red-circles due to the lower RIN. However, the red-circles become less BER around middle part owing to a shorter-tailed noise distribution by the MZI. As illustrated in Fig. 5(c), we could also observe an effect of statistical noise distribution by measuring histograms for each injection power without signal modulation. Thus, the statistical noise distribution affects the BER performance more than average RIN.

#268199 Received 13 Jun 2016; accepted 14 Jun 2016; published 17 Jun 2016

3. Application to seeded DWDM system

3.1 10-Gb/s signal transmission based on local-seeding

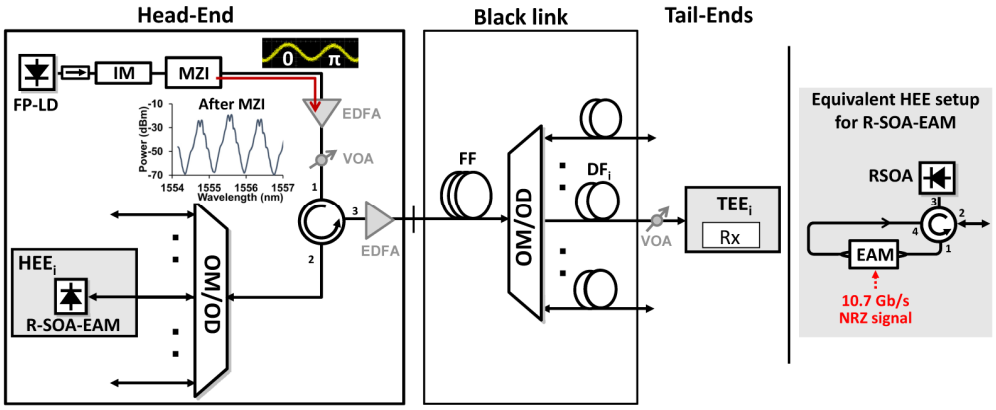

Fig. 6. Experimental setup for the 10-Gb/s signal transmission in DWDM system based on local-seeding (downstream signal transmission). Inset shows optical waveform of CS pulses, optical spectrum of CS pulse-modulated FP-LD, and an equivalent setup for an R-SOA-EAM.

Figure 6 shows the experimental setup for demonstrating a 10-Gb/s signal transmission in a DWDM system based on local-seeding (head-end to tail-end signal transmission or downstream signal transmission). This follows the previous experimental setup for the BER measurement described in Section 2. In the head-end, the FP-LD with the MZI is applied as a seed-light-source. It should be noted that a single MZI as well as an FP-LD would be shared by all DWDM channels for cost-effectiveness. Two 100 GHz channel spaced AWGs were utilized as an optical demultiplexer/multiplexer (OD/OM) in the head-end and the black link, respectively. Here the black link is composed of a feeder fiber (FF) and a number of drop fibers (DFs) as well as the AWG [14]. As mentioned before, an external intensity modulator (denoted as IM in Fig. 6) was inserted for pulse carving and it was realized by a single-drive or dual-drive $LiNbO_3$ intensity modulator. Especially, the dual-drive modulator enables to generate a carrier suppressed (CS) pulse train for a CS-RZ format. The inset of Fig. 6 shows a measured waveform and optical spectrum of the CS pulse train. In comparison to a conventional RZ50 signal (single-drive modulator case), the CS-RZ has a narrower spectral width resulting from 67% duty cycle and the relative phase of neighboring pulses differs by π [19–21]. These features have the CS-RZ format enhance dispersion tolerance of the system. In order to generate the CS pulse train, a bias voltage was set at the minimum transmission and the driving clock signal which has an amplitude of 2Vπ was applied to the modulator with half of bit-rate (5.35 GHz), where the Vπ is its half-wave voltage of 5.5V.

In a head-end equipment (HEE), the R-SOA-EAM for each user was comprised of a four ports circulator, RSOA and EAM as shown in inset of Fig. 6. It should be noted again that those components can be integrated by a compact R-SOA-EAM module [22]. Unfortunately, the used EAM in our demonstration has a large insertion loss of 17.5 dB under signal modulation. To compensate this, we utilized an additional EDFA to emulate a conventional EAM which has an insertion loss of 10 dB [23]. The EAM driven by an NRZ signal generates a 10.7-Gb/s RZ50 or CS-RZ signal by inputting the 50% or the CS pulsed-seed-light, respectively. The modulated signal then passed through two AWGs and the FF. After propagating through the DF, it was then delivered to an APD-based receiver in a tail-end equipment (TEE). In this demonstration, we did not use any dispersion compensating techniques thanks to a narrow spectral width of individual FP cavity modes.

#268199 Received 13 Jun 2016; accepted 14 Jun 2016; published 17 Jun 2016

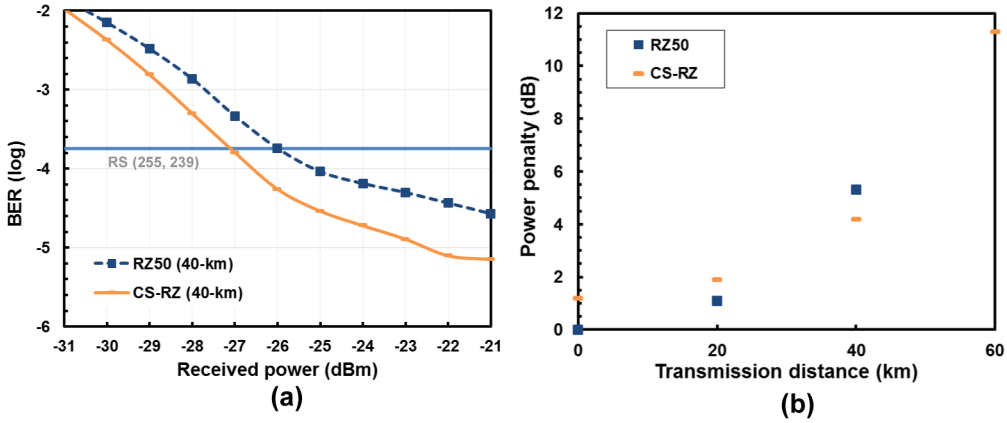

Fig. 7. (a) Measured BER curves after 40-km SMF transmission and (b) power penalty for RZ50 and CS-RZ signal versus fiber length.

Figure 7(a) shows the measured BER curves of the RZ50 and CS-RZ signal after 40-km SMF transmission. Based on the BER curves versus fiber length, power penalty was measured for evaluating the transmission performance at the FEC threshold according to a transmission distance. The BER curve for the RZ50 signal under a back-to-back (B-to-B) condition was considered as a reference (receiver sensitivity of −30.4 dBm). The injection power to the RSOA was set to be −6 dBm. Figure 7(b) shows that the CS-RZ signal has 1.2 dB power penalty compared with the RZ50 signal under the B-to-B condition. As referred to in [19], this is because the RZ50 signal has more high frequency components than the CS-RZ signal at the optical receiver which has a 6-GHz bandwidth. Thus, the RZ50 signal retains a pulse shape better than the CS-RZ signal. After 20-km SMF transmission, the RZ50 format shows still better BER performance. However, the CS-RZ format is more dispersion tolerant than the RZ50 format. The power penalty induced by fiber dispersion was less than 1 dB for CS RZ signal. The CS-RZ format gives the even better receiver sensitivity after a 40-km SMF transmission. The power penalties of the CS-RZ and RZ50 signal were measured to be about 4.2 dB (3 dB dispersion penalty plus 1.2 dB penalty under B-to-B condition) and 5.3 dB, respectively. Thus if we accepted 3-dB power penalty by the dispersion, the CS-RZ format would be selected for 40-km reach 10 Gb/s signal transmission.

3.2 10-Gb/s signal transmission based on remote-seeding

We also confirmed the feasibility of 10-Gb/s signal transmission based on a remote-seeding scheme (tail-end to head-end transmission or upstream signal transmission) as depicted in Fig. 8. In comparison to the local-seeding scheme, the differences are 1) a continuous wave (CW)-seed-light in the head-end was injected into the R-SOA-EAM at the TEE after propagating through the FF, AWG, and DF in the black link and 2) a 10.7-Gb/s RZ50 signal was electrically generated by an AND operation between a clock signal and NRZ signal and then applied to the EAM. The TEE has an additional EDFA after the EAM output to compensate its large insertion loss. The modulated signal from the TEE then delivered to the HEE receiver.

As with previous studies, a pulse-seeding technique gives an advantage of the less frequency chirping occurred in the EAM. In the case of remote-seeding, temporal broadening of the pulsed-seed-light would degrade the system performance though. Moreover, we may need a dynamic timing synchronization between the injected optical pulse and driving NRZ signal, since the coherence would be broken after pulse propagation over the optical fibers (FF and DF) in the black link. Thus, the electrical RZ50 signal was selected for the remote-seeding scheme.

#268199 Received 13 Jun 2016; accepted 14 Jun 2016; published 17 Jun 2016

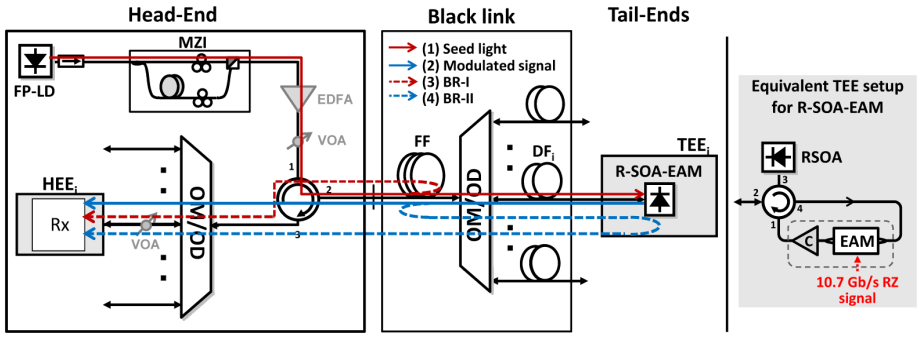

Fig. 8. Experimental setup for the 10-Gb/s signal transmission in DWDM system based on remote-seeding (upstream signal transmission). Inset shows an equivalent setup for R-SOA-EAM.

At the HEE, we measured BERs after the 20-km transmission. The electrical RZ50 signal was superior to the NRZ signal in spite of the wider signal spectrum (as referred to in [19], the RZ50 is 3/2 times the bandwidth of the NRZ), since the RZ50 signal has a wider timing margin and higher signal-to-noise-ratio (SNR) [4]. When the fiber length increased up to 40-km, the BER performance became worse and it was not able to achieve the FEC threshold for the both RZ50 and NRZ signals.

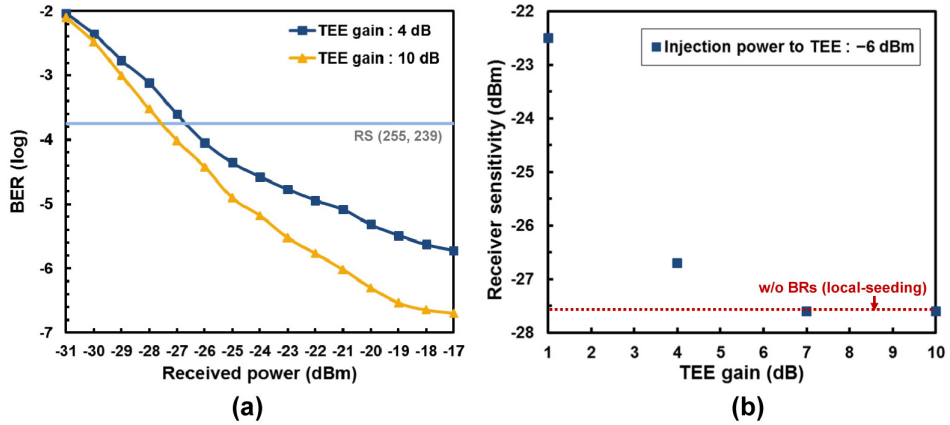

Fig. 9. (a) Measured BER curves for 10.7-Gb/s RZ50 signal and (b) receiver sensitivity according to TEE gain at −6 dBm injection power.

Figure 9(a) shows the measured BER curves for the 10.7-Gb/s RZ signal over the 20-km SMF when injection power to the TEE was −6 dBm. At this injection power, a fiber-to-fiber gain of the TEE was measured to be about 4 dB and thus output power of the transmitter was −2 dBm. The BER curve sufficiently satisfied the FEC threshold with receiver sensitivity of −26.7 dBm (■). It may be noted here that power budget and margin was 24.7 dB and 8.2 dB, respectively. Two AWGs, 20-km SMF, and circulator has an insertion loss of 11 dB, 4.5 dB, and 1 dB, respectively. As the TEE gain was increased up to 10 dB, the BERs improved by one order of magnitude at −18 dBm received power (▲).

The dependency on the TEE gain can be understood by an effect of an intrachannel crosstalk by Rayleigh back-reflections (BRs) in RSOA-based coherent remote-seeding [24]: the back-reflection of the injected seed light (red solid line in Fig. 8) to the HEE receiver, BR-I (red dashed line), and the back-reflection of the modulated signal (blue solid line) to the TEE transmitter, BR-II (blue dashed line). At the HEE receiver, these back-reflected lights interfere with the modulated signal, resulting in degradation of transmission performance. In

#268199 Received 13 Jun 2016; accepted 14 Jun 2016; published 17 Jun 2016

the low-TEE-gain region (≤ 10dB), the BR-I is more dominant than BR-II. The BR-I limited system shows that the larger gain TEE transmitter (▲) improves signal-to-crosstalk-ratio (SCR) and thus the BER performance becomes better. The SCR was measured to be 26 dB at the HEE receiver.

We then measured the receiver sensitivity at the FEC threshold to assess the effect of back-reflections in more detail. As seen in Fig. 9(b), a back-reflection-induced penalty dramatically increases with reducing the TEE gain to 1 dB. At the TEE gain of 7 or 10 dB, the back-reflection-induced penalty would be negligible (same BER performance with the local-seeding scheme). For these TEE gains in practical manner, we may need an additional high-output-power or high-saturation-power SOA [25] which can be integrated with an R-SOA-EAM. Of course, the high-output power SOA may increase the cost and power consumption. It should be noted that the TEE gain has to be less than 10 dB to prevent an effect of the BR-II.

3.3 Transmission of DWDM channels

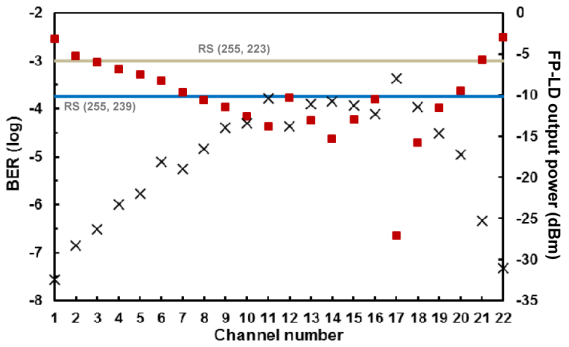

Fig. 10. Measured BER and FP-LD output power according to various DWDM channel.

In the previous experiments, we selected the best performance channel (# 17 mode). In order to count the number of useable DWDM channels (i.e., DWDM signal transmission) in the remote seeding scheme, we measured BER for other channels as shown in Fig. 10. For the fair comparison, injection power to the RSOA in a TEE transmitter as well as the received power at a HEE receiver was set to be same for all DWDM channels by adjusting VOAs in each BER measurement. As mentioned in Section 2.2, the noise reduction by the gain saturated RSOA strongly depends on the injection power. Thus, it gives a same noise reduction performance for all DWDM channels. The injection power and received power was −6 dBm (TEE gain of 10 dB) and −18 dBm, respectively. The MZI of course has a weak dependence versus the DWDM channel. Unfortunately, the result shows that the measured BERs have about four orders of magnitude difference. Since noise reduction ratio of the system is almost same according to DWDM channel, the BER variations are mainly attributed to noise characteristics of the FP-LD before noise reduction. As referred to in [26], the higher output power mode tends to have lower mode partition noise. This reverse relationship is clearly observed by comparing the measured BER results with the output power of the FP-LD. Nonetheless, twelve channels were available with the use of the RS (255, 239) code. If we used the RS (255, 223) considered as a suitable FEC code for the 10G-EPON [27], eighteen channels would be available with the increased FEC overhead. Future optimization of gain of the FP-LD is aimed at reducing intensity variations among individual FP cavity modes. Then more DWDM channel would be useable with enough BER margin.

4. Discussion and Conclusion

For the practical deployment of pulse-seeding system, we need to consider an effect of ambient temperature changes on the MZI. The SMF which comprises the MZI changes

#268199 Received 13 Jun 2016; accepted 14 Jun 2016; published 17 Jun 2016

refractive index as 0.000012/°C [28]. Then time delay change is expected about picosecond range due to temperature change. It would be negligible compared to the initial time delay of 50 ns. However, when a pulse-seeding scheme was utilized, the temporal mismatch of the RZ or CS-RZ pulses at the output of the MZI would degrade the transmission performance. If the 2-dB power penalty is permitted, about 20 ps mismatch can be allowable [6]. It implies that temperature change of 50 °C can be acceptable, considering the index change coefficient of 0.000012/°C.

In conclusion, we have described how to reduce the mode partition noise of a spectrally sliced FP-LD by using the MZI and the gain-saturated RSOA. We confirmed that the MZI was able to reduce the intensity noise more than 3 dB and change its distribution. The noise distribution change as well as noise reduction brings about a significant BER improvement by three orders of the magnitude for the 10-Gb/s signal.

By employing the proposed the noise suppression method, 10-Gb/s signal transmission in an injection seeded DWDM system has been demonstrated. In the experiment, any dispersion compensation techniques were not required due to the narrow linewidth of an individual FP cavity mode. For the signal transmission from HEE to TEE (local-seeding), an optical RZ50 format generated by inputting a pulsed-seed-light (pulsed FP-LD) to an NRZ-driven HEE transmitter is preferable for reach of 20-km. When the transmission distance is longer than 20-km, a CS pulsed-seed-light source will provide a better performance. On the other hand, for the TEE to HEE transmission (remote-seeding), a CW-seed-light (CW FP-LD) can be injected to a TEE transmitter driven by an electrical RZ50 signal. The reason for use of the CW-light-seeding is 1) to avoid penalty arising from the broadening of the pulsed-seed-light by dispersion and 2) to eliminate dynamic timing synchronization to seed light and the driving signal.

Furthermore, we compare the proposed system with other deployable DWDM passive optical networks (PONs) based on electro-absorption modulated lasers (EMLs) and ASE injection seeding [5,29]. The EML-based system shows the superior transmission performance (e.g., achievable bit-rate, distance) among those solutions due to low noise and narrow linewidth. However, each end-user (both HEE and TEE) requires not only a rather expensive EML and but also a fine tuning control of wavelength for channel assignment and maintenance. ASE injection seeded DWDM PONs, meanwhile, can support a colorless or color-free operation (automatic wavelength control). In addition, we believe an R-SOA-EAM for each user as a reflective modulator could be implemented with a cost-effective manner with respect to the EML in manufacturing process (low-cost EAM which has a high chirp parameter can be integrated for the R-SOA-EAM due to pulse seeding). However, this incoherent system is limited by ASE-ASE beat noise and vulnerable to chromatic dispersion of transmission fiber. Thus, dispersion compensation techniques are mandatory. The proposed system has a great tolerance against dispersion and support a colorless operation controlling temperature of one FP-LD. A simple MZI should be used for reduction of mode partition noise. A RZ signal transmission improves a system performance more with the cost of pulse carving (including timing synchronization).

The proposed noise suppression technique could be more effective for an advanced multi-level modulation format such as a four-level pulse amplitude modulation (PAM4) which is sensitive to the intensity noise [30].

Acknowledgments

This work was partly supported by Institute for Information & communications Technology Promotion (IITP) grant funded by the Korea government (MSIP) [B0101-15-1346, Development of Port-agnostic optical transceiver for Metro-SDN] and [R0166-15-1016, Standardization of colorless metro WDM technology].

#268199 Received 13 Jun 2016; accepted 14 Jun 2016; published 17 Jun 2016